Biochemical Engineering Journal 79 (2013) 57–70

Contents lists available at SciVerse ScienceDirect

Biochemical Engineering Journal

journal homepage: www.elsevier.com/locate/bej

Five-step continuous production of PHB analyzed by elementary flux, modes, yield space analysis and high structured metabolic model

Markan Lopar[a], Ivna Vrana Špoljarić[a], Aid Atlić[b], Martin Koller[b], Gerhart Braunegg[b], Predrag Horvat[a,*]

[a] Department of Biochemical Engineering, Faculty of Food Technology and Biotechnology, University of Zagreb, Pierottijeva 6/IV, HR-10000 Zagreb, Croatia
[b] Institute of Biotechnology and Biochemical Engineering, Graz University of Technology, Petersgasse 12, A-8010 Graz, Austria

ARTICLE INFO

Article history:
Received 25 February 2013
Received in revised form 5 July 2013
Accepted 8 July 2013
Available online xxx

Keywords:
Cupriavidus necator
Elementary modes
High-structured mathematical model
Metabolic fluxes
poly(3-Hydroxybutyrate)
Yield space analysis

ABSTRACT

A high structured metabolic model for PHB synthesis by *Cupriavidus necator* DSM 545 consisting of 43 mass balance equations related to the same number of intracellular compounds was established. The metabolic state of cells cultivated in a continuously operated five stage bioreactor cascade was analyzed by help of elementary flux modes and two-dimensional yield space. Two different C-source feeding strategies were performed. Concerning PHB and biomass yields, values of the more efficient strategy were used as the data source for elementary modes and metabolic flux calculations, respectively. Metabolic fluxes were calculated from experimental yield data using a combination of elementary modes by applying the quadratic programming approach, in which the sum of squared weighting factors was minimized. Two different metabolic situations concerning activity of glucose-6-phosphate isomerase were tested. The high structured metabolic model was validated by comparison of experimental data from 24 h batch cultivation and simulated results.

1. Introduction

Poly(hydroxyalkanoates) (PHAs) are biodegradable intracellular polyesters synthesized by various eubacterial genera and several archaea [1–3] with a variety of important functions in various ecosystems [4], mainly serving as an intracellular energy- and C source reservoir [5]. The homopolyester poly([*R*]-3-hydroxybutyrate) (PHB) is the best characterized and most intensively investigated type among a great number of known different PHAs. By methods of industrial biotechnology (recently known as "white biotechnology") they can be produced from renewable resources of first and second generation (lignocelluloses wastes, grains, beet and cane sugar, whey, biodiesel and biodiesel waste, i.e. glycerol and waste lipids) [6–8]. These polyesters can be separated from the surrounding microbial cells and, after appropriate processing, they can serve as biodegradable substitutes for petrochemical plastics such as poly(ethylene) (PE) and poly(propylene) (PP) [9–12].

Considering their production costs and some material properties, PHAs are still inferior to petro-chemically originated plastics [13–15], but recent oil price fluctuation lead to increased attention for these biopolymers. Continuous production based on renewable resources is a promising tool for the reduction of production costs and for improving sustainability aspects in PHAs life cycle.

The first experiments dealing with continuous production of PHAs performed in a one stage chemostat system [16,17] were followed by experiments of Koyama and Doi [18] as well as by Yu et al. [19]. In these experiments, the applied dilution rate was found as the most important factor influencing number-average molecular mass (M_n) of PHAs (decisive for the processing properties). Three different types of microbial producers were reported in the past concerning PHA production kinetics:

(i) Strains that express strict separation between growth phase and PHA production phase under N or P limitation (i.e. *Pseudomonas* sp. 2F, *Methylomonas extorquens* [20]).
(ii) Strains that accumulate PHA to a certain extent under balanced nutritional conditions and amplified PHA accumulation in non-growth phase caused by N or P limitation (i.e. *Cupriavidus necator*).
(iii) Strains that feature high formation rates for PHA even without any limitation of an essential growth component (i.e. *Azahydromonas lata* DSM 1122 [2,21], *Pseudomonas putida* GPo1 ATTC 29347 [2,22,23].

For the microorganisms mentioned under (i) and (ii) it was reasonable to apply two stage continuous cultivation where the first

* Corresponding author. Tel.: +385 1 46 05 166; fax: +385 1 48 36 424.
E-mail addresses: mlopar@pbf.hr (M. Lopar), ivrana@pbf.hr (I. Vrana Špoljarić), aid.atlic1@gmail.com (A. Atlić), martin.koller@tugraz.at (M. Koller), g.braunegg@tugraz.at (G. Braunegg), phorvat@pbf.hr (P. Horvat).

1369-703X/$ – see front matter © 2013 Elsevier B.V. All rights reserved.
http://dx.doi.org/10.1016/j.bej.2013.07.003

stage was intended for extensive biomass growth and the second stage for non growth-associated PHA synthesis as well as for achieving of appropriate molecular mass [24–28].

Chemostats have been used in the past also for special purposes i.e. investigation of C/N ratio as regulating factor of PHA synthesis [29–33].

Recently Atlić et al. [34] have tested a five stage continuous process constructed to achieve different but tailored process conditions in each step of the cascade, regarding types and concentrations of substrates and co-substrates as well as parameter values like temperature, pH-value and dissolved oxygen. This "cascade" strategy was chosen in order to act as a suitable tool for designing novel biopolymers for special applications, e.g. block-polymers [35] with alternating "soft" and "hard" segments or polymers with desired molecular mass and controlled polydispersity index.

The five-stage system was intended to provide a complete nutrient supply in the first reactor (balanced biomass growth), furthermore, the subsequent, second vessel was intended to complete the consumption of nitrogen source (growth-associated PHA synthesis), the aim of the last three reactors was to force the cells to non-growth associated synthesis of PHA under nitrogen-free, but C-source reach conditions. In addition, it was expected from the mentioned five stage system to provide information about cells tolerance to long term N-limitation (concerning cell damages and loss of the PHA synthesis). This way, from the bioprocess engineering point of view, each of the three different metabolic states of the production strain *C. necator* was reflected by different stage of the technological reactor system.

Furthermore, the just mentioned five stage bioreactor system was optimized by Horvat et al. using low structured, formal-kinetic mathematical model [36]. However, the applied low structured kinetic model was not able to predict the transient states between three different metabolic states, and, therefore, its achievements were limited. It is possible to solve such problems by applying high structured mathematical models of metabolic networks. In this work the reconstruction of metabolic network for *C. necator* DSM 545 was based on genome structure and data originated from databases as GeneDB, Kyotto Encyclopedia of Genes and Genomes (KEGG), BioSilico, University of Minnesota Biocatalyst/Biodegradation Database (UMBBD), Transport DB, ExPASy, BRENDA.

The five-step continuous process was analyzed by metabolic engineering methods as useful tools for getting a deeper insight into the metabolic and physiological situations of the cells in each step of the reactor system. Metabolic engineering methods described by Stephanopoulos et al. [37] as well as by Gombert and Nielsen [38] were additionally improved and new approaches have been developed for analysis of complex metabolic networks: flux balance analysis [39–41], elementary (flux) mode analysis [41,42], extreme pathways approach [43–45], flux variability analysis [46,47], minimal metabolic behaviors [48] and dynamic simulation and parameter estimation [49].

Elementary modes (EMs) are the smallest sub-networks that allow a metabolic reconstruction network to operate under steady state conditions [42]. EMs defined as a set of vectors that originate from the stoichiometric matrix of a metabolic network are characterized by three main properties:

(a) In a given network a unique set of elementary modes exists.
(b) 'Non-decomposability' means that any removed reaction in any elementary mode consequently excludes the whole elementary mode, so it cannot operate as a functional unit.
(c) All routes through a metabolic network consistent with property (b) are parts of elementary modes set.

In complex metabolic networks the combinatorial overproduction of number of EMs is possible. In such cases, by using "yield analysis" (YA) the "overproduced" set of EMs can be reduced to a minimal subset of EMs that is able to describe the related metabolic situation [50]. The solution space in yield analysis of metabolic pathways is a bounded convex hull in the yield space. Relative metabolic fluxes for the whole network of pathways can be calculated by appropriate software. In this work the elementary modes concept and metabolic yield analysis were applied in order to analyze metabolic situations in PHB producing cells in all steps of the continuous five stage process. According to our knowledge, this is the first time that a high structured metabolic model, the elementary modes concept and metabolic yield analysis were applied together for analyzing of continuous multistage production of PHB.

2. Materials and methods

2.1. Five-stage bioreactor cascade

The continuous cascade system consisting of five bioreactors is shown in Fig. 1. The cultivation procedures, as well as the information regarding fermentation experiments and obtained results were described earlier by Atlić et al. [34]. Briefly, in the first 23 h the

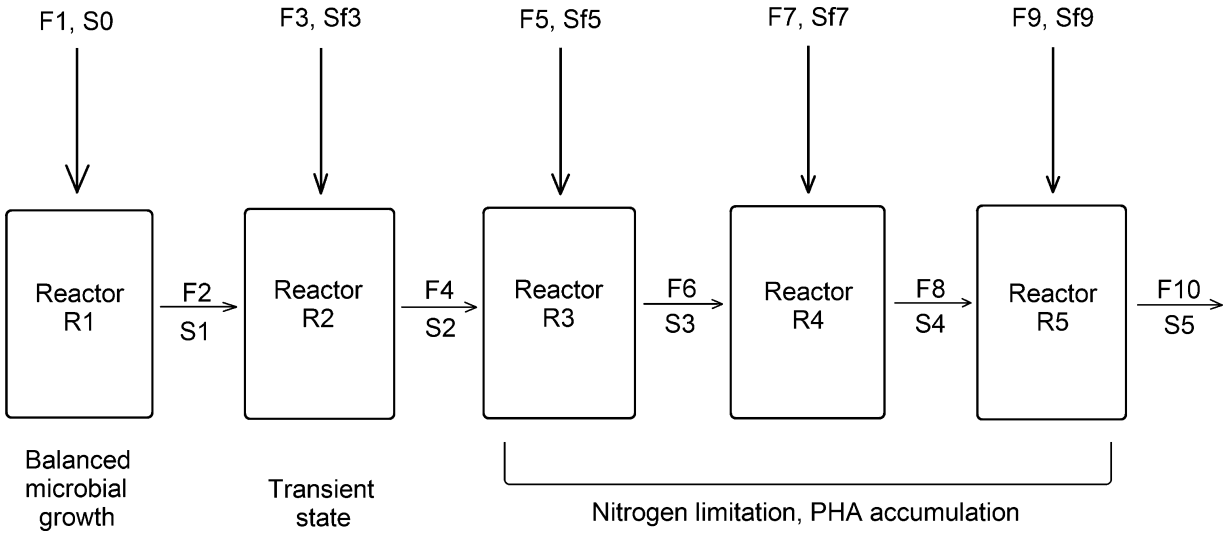

Fig. 1. Five-step bioreactor cascade for continuous PHB production.

fermentation is conducted in batch mode and only in the first reactor. After 23 h the grown biomass is distributed to each of the five reactors in the cascade and the fermentation is switched to continuous mode. Concentration of ammonium sulphate at the beginning of the batch part fermentation was 8.0 g/L., while in continuous part of fermentation NH_4OH was added in the first reactor automatically (to keep the pH constant). In all reactors of the cascade the set points for pH were adjusted to value 6.8, for temperature to value 30 °C, and for dissolved oxygen to value 27 (reactor 1), 17 (reactor 2), 20 (reactors 3 and 4) and 13% (reactor 5) of saturation respectively. The cultivations were performed under aerobic conditions, dissolved oxygen concentration was regulated by automatic adjustment of stirrer agitation speed and air inflow (Table 1). KH_2PO_4 as the P-source was added only in the first reactor as the component (4.3 g/L) of the main feed stream (F1), intended to be in light surplus toward C and N source. Detailed description can be found in [34]. Two types of continuous fermentations differing in the C-substrate (glucose) feeding strategy were performed (Table 1).

2.2. Analytical procedures

The analytical procedures for glucose, PHB, cell dry matter and ammonia were described in details elsewhere [34,36].

2.3. The metabolic network

The metabolic network for growth of *C. necator* DSM 545 on glucose is presented in Fig. 2. The necessary metabolic and transport data for metabolic network were retrieved from various databases: GeneDB, KEGG, BioSilico, UMBBD, TransportDB, ExPASy, BRENDA. In addition, some data concerning transport equations published in scientific articles were included [51,52] as well as data from Franz et al. [53] and Park et al. [54]. The established metabolic network consists roughly of phosphoenolpyruvate:sugar transpherase system, Embden–Meyerhof–Parnas and pentose phosphate pathway, Entner–Doudoroff pathway, tricarboxylic acid cycle, glyoxylate shunt, PHA synthesis and degradation pathways and paths for residual biomass formation. It consist 45 reactions in total. These metabolic reactions (presented below) were used for generating elementary (flux) modes and stoichiometric matrix by the software Metatool [55]. The reaction labels (r_1–r_{45}) match the ones presented in Fig. 2.

r_1: GLU + PEP → G6P + PYR.

r_2: G6P + NADP → 6PG + NADPH.

r_3: 6PG → KDPG.

r_4: KDPG → G3P + PYR.

r_5: 6PG + NADP → Ril5P + NADPH + CO_2.

r_6: Ril5P ↔ R5P.

r_7: Ril5P ↔ X5P.

r_8: R5P + X5P ↔ G3P + S7P.

r_9: G3P + S7P ↔ E4P + F6P.

r_{10}: X5P + E4P ↔ F6P + G3P.

r_{11}: G6P ↔ F6P.

r_{12}: F16P → F6P + Pi.

r_{13}: F16P ↔ G3P + DHAP.

r_{14}: DHAP ↔ G3P.

r_{15}: G3P + NAD + Pi ↔ BPG + NADH.

r_{16}: BPG + ADP ↔ 3PG + ATP.

r_{17}: 3 PG ↔ 2 PG.

r_{18}: 2 PG ↔ PEP.

r_{19}: PEP + ADP → PYR + ATP.

Table 1
Basic parameters in 5-stage continuous cultivation of *C. necator* (production of PHB from glucose).

Reactor	Feed inflow* [L h^{-1}]	Total inflow/outflow* [L h^{-1}]	Glucose concentration in the feed stream* [g/L]	Reactor volume, V_i [L]	Dilution rate, D_i [h^{-1}]	pH-value	Temp. [°C]	pO_2# [%] of saturation	Aeration# (flow rate) [L/min]	Stirring# [rpm]
Cultivation A										
1	$F_1 = 0.222$	$F_2 = F_1 = 0.222$	$S_0 = 67$	1.6	0.139	6.81 ± 0.01	30.0	26.76 ± 9.74	17.3 ± 1.8	896 ± 12
2	$F_3 = 0.0196$	$F_4 = F_2 + F_3 = 0.2416$	$S_{f3} = 500$	1.63	0.148	6.78 ± 0.12	30.0	17.32 ± 6.78	2.0 ± 0.0	796 ± 48
3	$F_5 = 0.0223$	$F_6 = F_4 + F_5 = 0.2639$	$S_{f5} = 500$	1.66	0.159	6.84 ± 0.03	30.0	20.0 ± 0.0	2.0 ± 0.0	740 ± 21
4	$F_7 = 0.0219$	$F_8 = F_6 + F_7 = 0.2858$	$S_{f7} = 500$	1.71	0.167	6.83 ± 0.02	30.0	20.0 ± 0.0	2.0 ± 0.0	756 ± 17
5	$F_9 = 0.0205$	$F_{10} = F_8 + F_9 = 0.3603$	$S_{f9} = 500$	2.36	0.130	6.81 ± 0.05	30.0	13.25 ± 9.79	2.0 ± 0.0	851 ± 46
Cultivation B										
1	$F_1 = 0.1587$	$F_2 = F_1 = 0.1587$	$S_0 = 70$	1.16	0.137	6.81 ± 0.04	30.0	38.28 ± 6.48	13.91 ± 1.60	884 ± 38
2	$F_3 = 0.0341$	$F_4 = F_2 + F_3 = 0.1928$	$S_{f3} = 536.8$	1.36	0.142	6.83 ± 0.06	30.0	16.0 ± 8.43	3.36 ± 0.81	838 ± 88
3	$F_5 = 0$	$F_6 + F_4 + F_5 = 0.1928$	$S_{f5} = 0$	1.3	0.148	6.93 ± 0.07	30.0	15.58 ± 7.85	3.94 ± 1.02	821 ± 109
4	$F_7 = 0.0253$	$F_8 = F_6 + F_7 = 0.2181$	$S_{f7} = 523.5$	1.36	0.160	6.82 ± 0.06	30.0	12.73 ± 10.09	3.73 ± 1.01	843 ± 66
5	$F_9 = 0$	$F_{10} = F_8 + F_9 = 0.2181$	$S_{f9} = 0$	1.13	0.193	6.92 ± 0.13	30.0	15.73 ± 8.49	3.55 ± 0.93	729 ± 147

* For detailed positions of inflows/outflows (F_1–F_{10}) and related glucose concentrations in the feed streams (S_0–S_{f9}), see Fig. 1.
\# The cultivations were performed under aerobic conditions, dissolved oxygen concentration was regulated by automatic adjustment of stirrer agitation speed and air inflow.

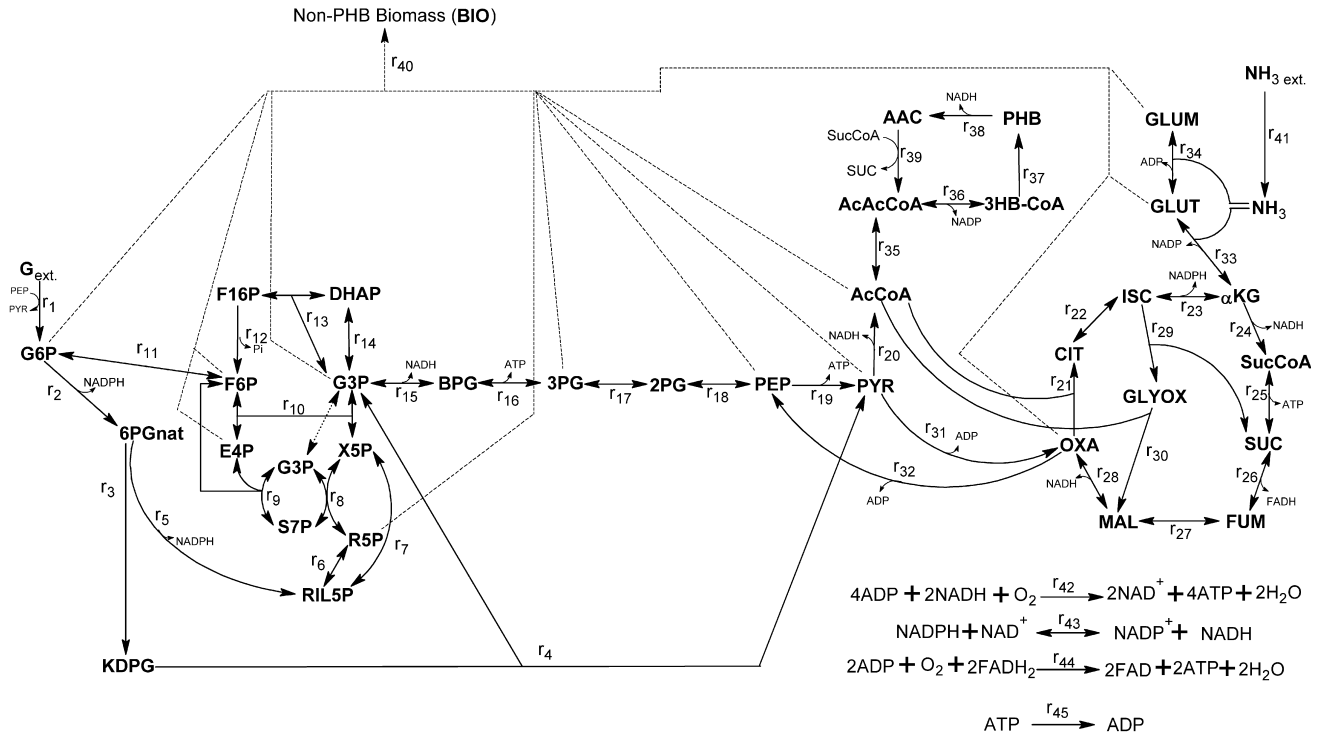

Fig. 2. Metabolic network of *C. necator* for growth on glucose.
AAC (acetoacetate); AcCoA (acetyl-coenzyme A); AcAcCoA (Acetoacetyl-coenzyme A); ADP (adenosine diphosphate); ATP (adenosine triphosphate); BIO (residual biomass); BPG (1,3-diphosphoglycerate); CoA (coenzyme A); CIT (citrate); DHAP (dihydroxy-acetonephosphate); E4P (erythrose-4-phosphate); FAD (flavin adenine dinucleotide); $FADH_2$ (reduced form of FAD); F6P (fructose-6-phpsphate); F16P (fructose-1,6-biphosphate); FUM (fumarate); G (glucose); G6P (glucose-6-phosphate); G3P (glycerol-3-phosphate); GLUT (glutamate); GLUM (glutamine); GLYOX (glyoxylate); Ril5P (ribulose-5-phosphate); ISC (isocitrate); KDPG (2-keto-3-deoxy-6-phosphogluconate); αKG (alpha ketoglutarate); MAL (malate); NAD (nicotinamide adenine dinucleotide); NADH (reduced form of NAD); NADP (nicotinamide adenine dinucleotide phosphate); NADPH (reduced form of NADP); OXA (oxaloacetate); PEP (phosphoenolpyruvate); PHB (poly(3-hydroksybutyrate); Pi (phosphate); PYR (pyruvate); S7P (sedoheptulose-7-phosphate); R5P (ribose-5-phosphate); SUC (succinate); SucCoA (succinyl-CoA); X5P (xylulose-5-phosphate); 2 PG (2-phosphoglycerate); 3HBCoA (3-hydroxybutyryl coenzyme A); 3 PG (3-phosphoglycerate); 6PGnat (6-phosphogluconate);; EXT subscript (external, extracellular).

r_{20}: PYR + NAD + CoA → AcCoA + NADH + CO_2.

r_{21}: AcCoA + OXA → CIT + CoA.

r_{22}: CIT ↔ ISC.

r_{23}: ISC + NADP ↔ aKG + NADPH + CO_2.

r_{24}: aKG + CoA + NAD → SucCoA + CO_2 + NADH.

r_{25}: SucCoA + ADP + Pi ↔ SUC + CoA + ATP.

r_{26}: SUC + FAD ↔ FUM + $FADH_2$.

r_{27}: FUM ↔ MAL.

r_{28}: MAL + NAD ↔ OXA + NADH.

r_{29}: ISC → GLYOX + SUC.

r_{30}: AcCoA + GLYOX → MAL + CoA.

r_{31}: PYR + ATP + CO_2 → OXA + ADP + Pi.

r_{32}: OXA + ATP → PEP + ADP + CO_2.

r_{33}: aKG + NADPH + NH_3 ↔ GLUT + NADP.

r_{34}: GLUT + NH_3 + ATP ↔ GLUM + ADP + Pi.

r_{35}: 2AcCoA ↔ AcAcCoA + CoA.

r_{36}: AcAcCoA + NADPH ↔ 3HBCoA + NADP.

r_{37}: 3HBCoA → PHB ∗ + CoA.

r_{38}: PHB ∗ + NAD → AAC + NADH.

r_{39}: AAC + SucCoA → AcAcCoA + SUC.

r_{40}: 0.021G6P + 0.09R5P + 0.036E4P + 0.007F6P + 0.013G3P + 0.153PG + 0.052PEP + 0.283PYR + 0.179OXA + 0.832GLUT + 0.025GLUM + 0.374AcCoA + 4.11ATP + 0.312NAD + 0.826NADPH → BIO + 0.751aKG + 0.374CoA + 4.11ADP + 4.479Pi + 0.312NADH + 0.826NADP + 0.261CO_2.

r_{41}: NH_3ext → NH_3.

r_{42}: $2NADH + O_2 + 4ADP + 4Pi \rightarrow 2NAD + 4ATP$.

r_{43}: $NADPH + NAD \leftrightarrow NADP + NADH$.

r_{44}: $2FADH2 + O_2 + 2ADP + 2Pi \rightarrow 2FAD + 2ATP$.

r_{45}: $ATP \rightarrow ADP + Pi$.

---

* Except in PHB polymerase reaction, in all stoichiometric reactions the term PHB means PHB-monomer (3-hydroxybutyrate).

It is assumed that the main route for glucose transport across the cell wall and the plasma membrane is the phosphoenolpyruvate:sugar transpherase system (PTS) [52]. Glucose is set to be predominantly metabolized trough Entner–Doudoroff metabolic pathway, and pentose phosphate pathway is assumed to be the main source for DNA/RNA synthesis. A part of Embden–Meyerhof–Parnas pathway is proposed to be the parallel "bridge" for the metabolic C-flux toward TCA cycle and PHB synthesis. The Ac-CoA pool was foreseen to be the branching point of C-flux between TCA cycle and PHB synthesis. For balancing of "reduction power" (NAD/NADH and NADP/NADPH) the reaction r_{43} ($NAD(P)^+$ transhydrogenase reaction) was included. Respiratory chain and coupled ATP generation are represented by two reactions (r_{42} and r_{44}). Reactions r_{36} (acetoacetyl-CoA reductase) and r_{37} (polyhydroxybutyrate synthase) in chain, are "responsible" for the PHB synthesis from Ac-CoA. In contrary, r_{38} and r_{39} (3-oxoacid CoA-transferase) are necessary for PHB consumption as reserve, intracellular C-storage material when no external C-source is present. Biomass synthesis reaction (r_{40}) was adopted from [53,69].

2.4. Elementary modes

In the work at hand the presumption of a quasi-steady state of internal metabolites was applied for the exponential growth phase as well as for the non-growth PHB synthesis phase. The changes of internal metabolites concentrations are mathematically expressed as a system of differential equations in which the change of concentration of each metabolite is calculated as a sum of all incoming and outgoing fluxes. Since the quasi-steady state presumption implies no change of metabolite concentrations, the mentioned system of differential equations becomes a homogenous system of linear equations. This system is usually underdetermined and as such it has an infinite number of solutions, most of which are biologically unfeasible. In this work the concept of elementary flux modes is applied for obtaining biologically feasible solutions. An elementary mode is defined as a minimal subset of reactions from metabolic network that can operate at steady state. This subset cannot be decomposed into smaller subsets, and by eliminating any reaction from this subset, a metabolic system cannot operate in steady state anymore. Elementary modes are calculated from stoichiometric matrix (which contains the stoichiometric coefficients for reactants and products) obtained from a given set of metabolic reactions (see Section 2.3), and the whole procedure is described elsewhere. [42,56]. More details about obtaining elementary modes for a given metabolic network and applying them in modeling can also be found in [43,53,55,56,68].

2.5. Metabolic yield analysis

From each elementary mode an overall reaction containing substrates (glucose, ammonia, oxygen) and products (residual biomass, PHB, CO_2) with related stoichiometric coefficients was obtained. The overall reaction of metabolic network is obtained by multiplying the stoichiometric coefficient of each external metabolite (from the set of reactions in Section 2.3) by calculated elementary mode coefficient of reaction in which that particular substance takes part (the list of all elementary mode coefficients can be found in file "Elementary modes.txt" under the section "enzymes"). These stoichiometric coefficients were further normalized with respect to the main substrate (glucose) thus obtaining the amount of products per unit of this substrate. The normalized stoichiometric coefficients were represented in yield space as described by Song and Ramkrishna [50]. From the geometrical point of view an unbounded polyhedral convex cone from the flux space is projected onto the yield space resulting in bounded convex hull.

As mentioned earlier, glucose is taken as reference substrate, so the elementary modes are represented in three-dimensional yield space ($Y_{BIO/GLU}$, $Y_{PHB/GLU}$, $Y_{N/GLU}$) because oxygen and CO_2 can be neglected. However, the dimensionality of this yield space was further reduced due to the fact that residual biomass is experimentally as well as stoichiometrically correlated to the consumed nitrogen source; hence the dimension $Y_{N/GLU}$ was excluded. As a result, our yield space has two dimensions ($Y_{BIO/GLU}$, $Y_{PHB/GLU}$). The calculated yields of PHB and residual biomass were used for obtaining a convex hull in the ($Y_{BIO/GLU}$, $Y_{PHB/GLU}$) yield space.

2.6. Calculation of experimental yields

The yields of residual biomass and PHB per glucose are calculated from available experimental data. For the batch part of fermentation this is accomplished by dividing masses of produced biomass and PHB by mass of consumed glucose after 23 h since the start of fermentation:

$$Y_{PROD/GLU} = \frac{\Delta m_{PROD}}{\Delta m_{GLU}} \tag{1}$$

where PROD denotes PHB or residual biomass BIO.

For the continuous part of fermentation, produced PHB and residual biomass were calculated for each bioreactor as follows:

$$\begin{bmatrix} \Delta m_{PHB,1} & \Delta m_{BIO,1} \\ \Delta m_{PHB,2} & \Delta m_{BIO,2} \\ \Delta m_{PHB,3} & \Delta m_{BIO,3} \\ \Delta m_{PHB,4} & \Delta m_{BIO,4} \\ \Delta m_{PHB,5} & \Delta m_{BIO,5} \end{bmatrix} = diag(t) \cdot \begin{bmatrix} F_2 & 0 & 0 & 0 & 0 \\ -F_2 & F_4 & 0 & 0 & 0 \\ 0 & -F_4 & F_6 & 0 & 0 \\ 0 & 0 & -F_6 & F_8 & 0 \\ 0 & 0 & 0 & -F_8 & F_{10} \end{bmatrix} \cdot \begin{bmatrix} PHB_1 & BIO_1 \\ PHB_2 & BIO_2 \\ PHB_3 & BIO_3 \\ PHB_4 & BIO_4 \\ PHB_5 & BIO_5 \end{bmatrix} \tag{2}$$

where $\Delta m_{PHB,i}$ and $\Delta m_{BIO,i}$, $i = 1, 2, 3, 4, 5$ are masses of PHB and residual biomass in each reactor R_i, respectively, PHB_i and BIO_i are steady state concentrations of PHB and residual biomass in each reactor R_i, respectively, $\boldsymbol{t} = [\Delta t_1\ \Delta t_2\ \Delta t_3\ \Delta t_4\ \Delta t_5]^T$ is the vector of steady state time intervals in each reactor R_i, and F_j, $j = 2, 4, 6, 8, 10$ are flows that are labeled the same way as in Fig. 1 and Table 1.

In the case of consumed glucose a feed inflow must also be accounted:

$$\begin{bmatrix} \Delta m_{GLU,1} \\ \Delta m_{GLU,2} \\ \Delta m_{GLU,3} \\ \Delta m_{GLU,4} \\ \Delta m_{GLU,5} \end{bmatrix} = diag(t) \cdot \left(\begin{bmatrix} -F_2 & 0 & 0 & 0 & 0 \\ F_2 & -F_4 & 0 & 0 & 0 \\ 0 & F_4 & -F_6 & 0 & 0 \\ 0 & 0 & F_6 & -F_8 & 0 \\ 0 & 0 & 0 & F_8 & -F_{10} \end{bmatrix} \cdot \begin{bmatrix} GLU_1 \\ GLU_2 \\ GLU_3 \\ GLU_4 \\ GLU_5 \end{bmatrix} + diag(F) \cdot \begin{bmatrix} S_0 \\ S_{f3} \\ S_{f5} \\ S_{f7} \\ S_{f9} \end{bmatrix} \right) \quad (3)$$

Here, $\Delta m_{GLU,i}$ and GLU_i, $i = 1, 2, 3, 4, 5$ are masses and steady state concentrations of glucose in each reactor R_i, respectively, $\mathbf{F} = [F_1\ F_3\ F_5\ F_7\ F_9]^T$ is the vector of glucose feed inflows from Fig. 1 and Table 1, and S_0, S_{f3}, S_{f5}, S_{f7} and S_{f9} are glucose feed inflow concentrations from Fig. 1 and Table 1.

2.7. Metabolic flux calculations

The obtained experimental yields that fall inside the convex hull were represented in the yield space as a linear combination of elementary modes. In order to represent experimental data with linear combination of elementary modes, each mode has a weighting factor assigned to it. Weighting factors calculated in this procedure are non-negative [57] and normalized to first order unit-norm [50]. A unique solution was obtained applying the quadratic programming approach [50,57,58], in which the sum of squared weighting factors was minimized. This approach favors those modes whose yield data in the yield space are closer to experimental yield data.

Metabolic fluxes of reactions network (Fig. 2) were calculated from experimental yields. Two different metabolic situations were considered concerning the key metabolic branch point (the glucose-6-phosphate node; r_1, r_2 and r_{11}, i.e. phosphoenolpyruvate sugar transpherase system/PTS/, 6-phosphogluconolactonase/glucose-6-phosphate dehydrogenase, glucose-6-phosphate isomerase reactions node). The first one was characterized by presence of all EMs when both flux directions of glucose-6-phosphate isomerase ("reversible" enzyme that catalyzes the synthesis of fructose-6-phosphate from glucose-6-phosphate) are allowed. In the second case it was assumed that mentioned enzyme catalyzes the formation of fructose-6-phosphate from glucose-6-phosphate ($r_{11} > 0$) when *C. necator* grows on glucose. Each pair of biomass-PHB yields in reactors R1–R5 (different cultivation conditions) was used for calculation of respective metabolic fluxes.

2.8. Validation of mathematical model

Based on the metabolic network in Fig. 1 a high structured metabolic model was established, which consists of 43 mass balance equations related to the same number of intracellular compounds. The mass balance equations for intracellular metabolites are presented in the supplementary file "Mass balance equations.doc". The reaction rate terms (kinetic equations, r_i) were adapted from the following literature data: Altintas et al. [59], Bruggeman et al. [60], Burns et al. [61], Chassagnole et al. [62], Hoefnagel et al. [63], Shi et al. [64], Usuda et al. [65], Yang et al. [66] and Yuan et al. [67]. These rate equations are provided in the supplementary file "Kinetic rate equations.doc". The built metabolic model was combined with a macro-kinetic model related to substrate and product concentrations for batch and continuous cultivation in bioreactor. Related equations for this macro-kinetic model are submitted as supplementary file "Mass balance equations.doc". The whole mathematical model was validated by comparison of simulated results and experimental data for batch cultivation of *C. necator* on glucose. Kinetic parameters (related constants) are presented in the supplementary file "Kinetic constants.doc".

2.9. Software tools

Stoichiometric matrix and elementary modes are calculated using the program Metatool, version 5.1 (http://pinguin.biologie.uni-jena.de/bioinformatik/networks/metatool/metatool5.1/metatool5.1.html) originally developed by Pfeiffer et al. [55] and further advanced by Kamp and Schuster [68]. This program consists of scripts written for Matlab software package (MathWorks Inc., Massachusetts, USA). The metabolic yield analysis is also performed using Matlab. Weighting factors are obtained using Matlab function fmincon.

3. Results and discussion

The total number of obtained elementary modes for the set of reactions (Section 2.3) and metabolic network presented in this paper (Fig. 2) is 916. These modes represent various states of the metabolic network. Below the overall reactions (computed from some of the elementary modes chosen from entire set as representative examples of metabolic properties of *C. necator*), are shown. Presented reactions demonstrate seven situations that may occur, when PHB producing microorganism exists in certain cultivation conditions, described in the number of literature references (water as product is neglected and biomass composition is $C_4H_{6.9}O_{1.64}N_{0.98}$ [69]):Consumption of glucose for maintenance energy without PHB synthesis and without biomass growth—that situation can occur when microorganism spends the whole quantity of PHB during glucose and nitrogen starvation, and afterwards the glucose is added in the system. One of 65 reactions of this type in total is presented below:

$$GLU + 6O_2 \rightarrow 6CO_2$$

PHB synthesis without biomass growth—this situation occurs usually when the exponentially growing microorganism is exposed to the nitrogen or phosphorus starvation, but in the presence of sufficient C-source. There are 18 such reactions in total and one of them is presented below:

$$4GLU + 15O_2 \rightarrow 2PHB\text{-monomer} + 16CO_2$$

Biomass growth without PHB synthesis—this type of reaction is characteristic for certain group of microorganisms which do not synthesize PHB when growing in complete broth (sufficient C-source, N, P, and other biogen elements). There are 206 such reactions and one example is presented below:

$$1.37445GLU + 1.20691NH_3ext + 2.33746O_2 \rightarrow 1.36835BIO + 2.78833CO_2$$

PHB synthesis with biomass growth—this type of behavior is characteristic for certain group of microorganisms which synthesize PHB in limited quantities when growing in complete broth. There are 30 such reactions of which the one is presented below:

$$1.91406GLU + 0.831543NH_3ext + 2.09399O_2 \rightarrow 0.942749BIO + 1.18201PHB\text{-}monomer + 2.99561CO_2$$

Biomass growth with glucose and PHB consumption—according to literature this is very rare situation. It can be present when glucose and other sources are present in small quantities and PHB was synthesized earlier. 503 such reactions are obtained and below is one example:

$$17.7354GLU + 30.169NH_3ext + 21.6415PHB\text{-}monomer + 56.0839O_2 \rightarrow 34.2053BIO + 56.5338CO_2$$

Biomass growth on PHB without glucose—this type of behavior happens frequently in the nature when C-source is depleted and other sources (e.g. nitrogen, phosphorus, etc.) are present along with already synthesized PHB. There are 62 such reactions in total of which the one is written below:

$$1.104NH_3ext + 1.99463PHB\text{-}monomer + 3.57037O_2 \rightarrow 1.25171BIO + 2.98547CO_2$$

PHB consumption without biomass growth—this type of behavior happens when C-source and other sources (e.g. nitrogen, phosphorus, etc.) are depleted and the cells consume already stored PHB for maintenance of cell structure. 32 such reactions are obtained and one is presented below:

$$PHB\text{-}monomer + 0.984375O_2 \rightarrow 0.875CO_2$$

The total number of elementary modes can be reduced if additional constraints are applied to the network. In our case, PHB consumption is not taken into consideration because it is expected that the cultivation conditions will be set to support and maximize PHB synthesis and yield, not its degradation. Therefore, the reactions r_{38} and r_{39} (PHB hydrolysis) can be eliminated from network, reducing the number of elementary modes from 916 to 164. In addition, it was reasonable to take into consideration those elementary modes that produce biomass, PHB or both (situations 2, 3 and 4) because one of its combinations is likely to be (concerning PHB and biomass yields) a possible solution for the investigated cultivation. There are 143 modes in total that represent the situations 2, 3 and 4. The set of obtained elementary modes is presented in the supplementary data file "Elementary modes.txt" (for both cases—without constraints and with constraint for flux of glucose-6-phosphate isomerase $r_{11} \geq 0$). Using the Metatool software, biomass and PHB yields ($Y_{PHB/GLU}$; $Y_{BIO/GLU}$) were calculated for all EMs originated from the basic metabolic network. These results are presented in two-dimensional yield spaces as dots in Figs. 3 and 4 where glucose is taken as reference substrate (because ammonia and biomass are stoichiometrically bound; 1 mol of used ammonia results in 11,338 mol of biomass for each elementary mode that produces biomass). In Figs. 3 and 4 it seems that the number of elementary modes is lesser than the reported number of 164. This is because some modes are overlapping in the yield space. Namely, many different elementary modes earn the same yield for residual biomass and PHB (because of existing parallel metabolic pathways such as EMP and Entner–Doudoroff pathway). The dashed line segments that connect the most outlying points form a convex hull that represents the solution space for the presented metabolic network. In Figs. 3 and 4, the experimental yields of biomass and PHB related to batch inoculum preparation as well as to all five reactors concerning continuous cultivation type A, considering both metabolic situations (related to isomerization of glucose-6-phosphate to fructose-6-phosphate), are provided.

Concerning yields of biomass and PHB (with respect to glucose), a remarkable situation occurs in cultivation A. Results presented in Figs. 3 and 4 clearly show different metabolic situations at different stages of the cascade. The yield data of the first reactor (intended to produce biomass in nutrient balanced medium) are positioned in the yield space very close to the $Y_{BIO/GLU}$ axis. This means that the biomass yield exceeds the product yield several times, and the possible solution in the yield space (for these two yields) can be achieved combining different EMs. In case of R1, the contribution of EMs directly located on the $Y_{BIO/GLU}$ axis will become dominant. Fairly different situation can be observed considering the second reactor (R2). The biomass yield (0.065 g/g) is significantly lower and

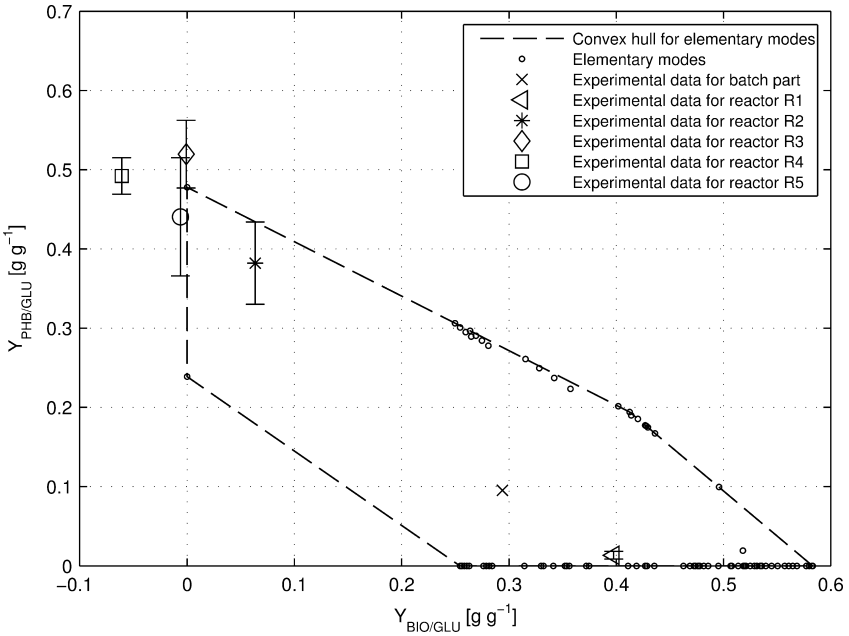

Fig. 3. Elementary modes and experimental yield data related to continuous five-step cultivation A in yield space ($Y_{PHB/GLU}$, $Y_{BIO/GLU}$) when no constraints are imposed (r_{11} can be bidirectional, i.e. positive or negative).

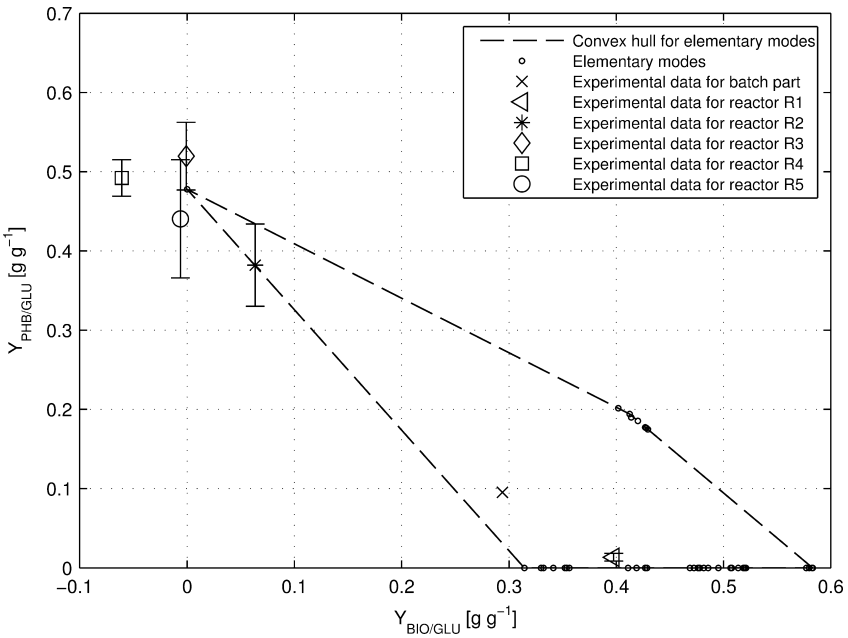

Fig. 4. Elementary modes and experimental yield data related to continuous five-step cultivation A in yield space ($Y_{PHB/GLU}$, $Y_{BIO/GLU}$) with imposed constraint $r_{11} \geq 0$ (G6P is converted to F6P or the reaction is in equilibrium).

the product yield (0.38 g/g) is much higher than in the first reactor. This is the consequence of lower nitrogen concentration in R2 because this source is dominantly consumed in the previous step R1 (there was no addition of NH_3 in reactors R2–R5), thus under the misbalanced C:N ratio, the C-flux is directed towards the synthesis of PHB instead of biomass. In both figures (Figs. 3 and 4) is possible to see that the left part of convex hull (biomass yields ranging from $0 < Y_{BIO/GLU} < \sim 0.25$/Fig. 3/or $0 < Y_{BIO/GLU} < 0.32$/Fig. 4/and PHB yield ranging from $0.25 < Y_{PHB/GLU} < 0.5$/Fig. 3/or $0 < Y_{PHB/GLU} < 0.5$/Fig. 4/) contains only a limited number of elementary modes (two in Fig. 3 and one in Fig. 4). That means that presented model offers only limited number of metabolic situations (combinations of EMs) related to the production of PHB without (or with very low) biomass synthesis (as in the nitrogen limited conditions). Much more possibilities are offered when the biomass yield is dominant and the PHB is synthesized as growth associated product (right part of the yield space). A similar situation was reported also for the cultivation of *C. necator* on fructose [53]. Highly remarkable results in the yield space were obtained for the last three reactors in the cascade (R3, R4 and R5). There was no synthesis of biomass in these reactors anymore (nitrogen starvation), so the biomass yields are positioned around zero and PHB yields surround the upper left corner of the yield space convex hull (Figs. 3 and 4). The upper left corner of the convex hull corresponds to the theoretical yield (0.478 g/g) of PHB per glucose, when the later one is metabolized through the Entner–Doudoroff pathway to acetyl-CoA and further through the intermediate 3-hydroxybutyrate to PHB. This means that under nitrogen starvation *C. necator* redirects C-flux toward PHB with high efficiency (practically close to the stoichiometric relation). Concerning the last three reactors in the cascade (R3, R4 and R5) and the yield space, it is necessary to clarify two uncertainties: the negative biomass yield in reactor R4 and product yield in reactor R3 that is higher than the theoretical one. The negative biomass yield displayed for R4 is an indication that under exposition of cells to insufficient nitrogen concentration in the second reactor and under nitrogen-free conditions in R3 and R4, the biomass starts to lyse. The biomass yield higher in R5 than in R4 might be the consequence of weak cryptic growth on the "own" hydrolyzate, but this obvious hypothesis was neither investigated in details nor confirmed by appropriate analytical procedures. It seems that the higher product yield in the reactor R3, even exceeding the theoretical value, is of minor concern because it can be considered as the consequence of PHB measuring accuracy. Namely, the theoretical PHB yield with respect to glucose ranges within the error bar corresponding to the PHB concentration measured in the third reactor (Figs. 3 and 4).

In the second experiment (cultivation B; results not shown), a different glucose feeding strategy compared to cultivation A was applied (Table 1); here, the reactors R3 and R5 were not supplied with additional glucose feed (Fig. 1; F5 and F9 = 0). In this case the first reactor has also dominantly converted the glucose to biomass, when compared with the low amount of produced PHB. On the contrary, the PHB production in reactors R2–R4 was dominant compared to biomass synthesis. Furthermore, in the last reactor (R5), a negative biomass yield coefficient with respect to the converted C-source was observed. This situation indicates the biomass degradation caused by long term nitrogen starvation (started in R3 and active in R4 and R5) that, in this experiment, is supported by low concentration of glucose (no feeding, F9 = 0). In general, when compared with cultivation A, this cultivation strategy has resulted in lower PHB yield from glucose and was not further investigated in details.

Different biomass and product yields achieved at the different stages (R1–R5) of the reactor cascade in both cultivations A and B indicate differences in metabolic flux distributions caused by altered C:N ratio. To indicate the differences in metabolic states of cells concerning the five reactors cascade, the overall reaction equations were obtained by the help of Matlab software using experimentally determined biomass and PHB yields as basis for the stoichiometric calculation (water was not taken in the account!):

Cultivation A

$$\text{Batch}: \ \text{GLU} + 0.4918\text{NH}_3 + 2.693\text{O}_2 \rightarrow 0.5576\text{BIO} + 0.1998\text{PHB-monomer} + 2.9766\text{CO}_2$$

$$\text{R1}: \ \text{GLU} + 0.6653\text{NH}_3 + 2.6164\text{O}_2 \rightarrow 0.7543\text{BIO} + 0.028\text{PHB-monomer} + 2.879\text{CO}_2$$

R2 : GLU + $0.1063NH_3 + 1.9013O_2$
→ $0.1205BIO + 0.7952PHB\text{-monomer} + 2.3386CO_2$

R3 : GLU + $1.5O_2$ → PHB-monomer + $2CO_2$

R4 : GLU + $1.5928O_2$ → $0.9794PHB\text{-monomer} + 2.0825CO_2$

R5 : GLU + $1.8518O_2$ → $0.9218PHB\text{-monomer} + 2.3127CO_2$

Cultivation B

Batch : GLU + $0.6994NH_3 + 1.0531O_2$
→ $0.7929BIO + 0.3384PHB\text{-monomer} + 1.4835CO_2$

R1 : GLU + $0.7252NH_3 + 2.0764O_2$
→ $0.8222BIO + 0.0829PHB\text{-monomer} + 2.3887CO_2$

R2 : GLU + $0.0373NH_3 + 2.4281O_2$
→ $0.0423BIO + 0.7531PHB\text{-monomer} + 2.8186CO_2$

R3 : -(notcalculatedbecauseofunexpectedhighPHByield!)

R4 : GLU + $0.1847NH_3 + 2.6914O_2$
→ $0.2094BIO + 0.5343PHB\text{-monomer} + 3.0275CO_2$

R5 : GLU + $2.7897O_2$ → $0.7134PHB\text{-monomer} + 3.1464CO_2$

Regarding the overall reactions of cultivation A, one can clearly distinguished between R1, R2 and the last three reactors R3–R5. The overall reaction in the first reactor is characterized by high production of biomass and coincides with the intended biological task of this reactor. The second reactor was intended to be the transient reactor; this task is indicated by enhanced PHB synthesis if compared to biomass. The overall reactions for the last three reactors are very similar in stoichiometric coefficients and correspond well to its envisaged purpose: no biomass synthesis but significant conversion of glucose towards PHB.

The yields achieved by the 5-stage cascade cultivation A that are presented in yield spaces in Figs. 3 and 4 were used as the source data for the calculation of fluxes of metabolic network (Fig. 1) by the software Metatool. Results are presented in Tables 2 and 3, respectively.

Here is important to note, that the applied software routine can offer multiple solutions concerning combinations of elementary modes and resulting yield pairs (for biomass and PHB). For example, two different metabolic situations were identified in sugar metabolism (flux of glucose-6-phosphate isomerase, r_{11}, bidirectional and unidirectional) that allow the same yield pairs in the yield space as they were achieved in the experiment. That means that this model is able to identify diverse metabolic possibilities and to give researches the guide mark for the focused research on the most probably metabolic points. In just mentioned case, both situations concerning r_{11} direction were considered in detail because they differ significantly in some reaction fluxes, especially in flux value and direction of r_{43} ($NAD(P)^+$ transhydrogenase). This reaction is important for the maintenance of NADH/NADPH ratio which is very influential on PHB synthesis. Figs. 3 and 4 clearly indicate that direction of glucose-6-phosphate isomerase reaction (r_{11}) significantly influenced the yield space. Calculated metabolic fluxes presented in Tables 2 and 3 clearly differ from each other, reflecting the different metabolic states of microbial cells in different stages of the cascade. The first observation is that metabolic fluxes of cells in R1 are in both cases (Tables 2 and 3) very similar to the fluxes of the batch part of cultivation. This is in good accordance with the fact that the batch part (inoculum preparation) was performed under nutrient balanced conditions; the same was the task of the first cascade reactor. The second observation that cannot be omitted is that, due to the fact that if r_{11} (glucose-6-phosphate isomerase reaction) is allowed to be bidirectional, some kind of futile cycle in sugar metabolism seems to exist (Table 2). This is indicated by the unusual situation that r_2, r_3, and r_4 fluxes (6-phosphogluconolactonase/glucose-6-phosphate dehydrogenase, phosphogluconate dehydratase, and 2-dehydro-3-deoxy-phosphogluconate aldolase reactions) are higher than the phosphoenolpyruvate:sugar transpherase system (PTS) flux (r_1) and, in addition, by the negative value of the flux for r_{11} (glucose-6-phosphate isomerase reaction). At the same time $NAD(P)^+$ transhydrogenase reaction (r_{43}) has changed the direction. Furthermore, the number of fluxes in penthose phosphate pathway (r_5–r_{14}) were changed for one or two orders of magnitude, r_7 (ribulose-phosphate 3-epimerase) and r_{10} (transketolase) have changed the direction, and the fluxes in the glyoxylate shunt were increased. On the contrary, if r_{11} (glucose-6-phosphate isomerase) is supposed to be positive (reaction direction G6P → F6P), the fluxes r_2 (6-phosphogluconolactonase/glucose-6-phosphate dehydrogenase), r_3 (phosphogluconate dehydratase), and r_4 (2-dehydro-3-deoxy-phosphogluconate aldolase) are lower than the PTS flux r_1 (Table 3). Which of these two metabolic situations occurs in reality can be only clarified by experimental determination of the mentioned fluxes. In addition, reactions r_{35}–r_{37} (PHB synthesis) are significantly higher for nitrogen limited reactors (R2, R3) for both cases (Tables 2 and 3) if compared with the nitrogen rich, biomass producing reactor R1. Furthermore, the fluxes r_{35}–r_{37} (PHB synthesis), r_{40} (biomass growth) and r_{41} (nitrogen uptake) are in the same order of magnitude in both investigated cases. Unfortunately, the points in the yield spaces related to R3, R4 and R5 (Figs. 3 and 4) are not located inside the convex hull (accuracy of analytical procedures and results dispersion); hence the exact calculation of metabolic fluxes for these three reactors was not possible. Therefore, the reactor R3 was taken into consideration by applying the lower value of error bars, and it is obvious that the three results related to R3, R4 and R5 which are close to the upper left corner of the convex hull are an expedient indicator of the high efficiency of PHB synthesis in these reactors, as they are close to the theoretical yield.

A high structured metabolic model was used for simulation of growth of *C. necator* under nutrient balanced conditions. It was assumed that under nutrient balanced growth conditions the microorganism will be in the exponential growth phase and that metabolic fluxes in the cells in this situation will be as high as possible. The experimental yield pairs achieved under these conditions lead to the EMs combination (and related metabolic fluxes) that satisfied maximal values of metabolic fluxes. It was supposed that these values can quantitatively cover the opposite metabolic situation, too: the PHB synthesis under nitrogen starvation. This way the model was validated by comparison of experimental results and simulated data concerning residual biomass and PHB concentrations (Fig. 5) as well as concerning the related yields.

The simulated results of nutrient balanced growth of *C. necator* obtained by high structured metabolic model are in highly satisfactory agreement with the experimental data. Experimental yields

Table 2
Metabolic fluxes ([mol S/mol Glu], normalized with respect to glucose uptake) related to different metabolic state of cells in 5-stage reactor cascade system (cultivation A) when r_{11} was assumed to be bidirectional, i.e. positive or negative.

	Batch	R1 yield			R2 yield			R3 yield
		Lower error value	Experimental value	Upper error value	Lower error value	Experimental value	Upper error value	Lower error value
r_1	1	1	1	1	1	1	1	1
r_2	1.557	1.383	1.396	1.398	2.11	2.035	1.873	1.867
r_3	1.199	1.104	1.1	1.107	1.481	1.579	1.835	1.867
r_4	1.199	1.104	1.1	1.107	1.481	1.579	1.835	1.867
r_5	0.3581	0.2791	0.2957	0.2902	0.6282	0.456	0.03782	0
r_6	0.1595	0.1473	0.1529	0.151	0.2181	0.1607	0.02128	0
r_7	0.1986	0.1318	0.1428	0.1392	0.4101	0.2953	0.01654	0
r_8	0.1093	0.07946	0.08499	0.08316	0.2072	0.1498	0.01044	0
r_9	0.1093	0.07946	0.08499	0.08316	0.2072	0.1498	0.01044	0
r_{10}	0.08926	0.0523	0.05784	0.056	0.2029	0.1455	0.0061	0
r_{11}	−0.5689	−0.3987	−0.4115	−0.4134	−1.112	−1.037	−0.8752	−0.867
r_{12}	0.3743	0.2722	0.274	0.2796	0.7028	0.7428	0.8595	0.867
r_{13}	−0.3743	−0.2722	−0.274	−0.2796	−0.7028	−0.7428	−0.8595	−0.867
r_{14}	−0.3743	−0.2722	−0.274	−0.2796	−0.7028	−0.7428	−0.8595	−0.867
r_{15}	0.5326	0.6018	0.6001	0.5945	0.2771	0.2371	0.1204	0.133
r_{16}	0.5326	0.6018	0.6001	0.5945	0.2771	0.2371	0.1204	0.133
r_{17}	0.449	0.4887	0.4869	0.4813	0.259	0.219	0.1023	0.133
r_{18}	0.449	0.4887	0.4869	0.4813	0.259	0.219	0.1023	0.133
r_{19}	2.184	1.796	1.771	1.726	2.568	2.382	1.719	2.201
r_{20}	1.89	1.75	1.716	1.698	1.892	1.798	1.867	2
r_{21}	0.6943	0.8071	0.781	0.762	0.2395	0.0876	0.01772	0
r_{22}	0.6943	0.8071	0.781	0.762	0.2395	0.0876	0.01772	0
r_{23}	0.1071	0.1815	0.1842	0.185	0.01282	0.01281	0.01279	0
r_{24}	0.04801	0.1015	0.1042	0.1051	4.663e−005	4.157e−005	1.776e−005	0
r_{25}	0.04801	0.1015	0.1042	0.1051	4.663e−005	4.157e−005	1.776e−005	0
r_{26}	0.6352	0.7271	0.7011	0.682	0.2267	0.07483	0.004955	0
r_{27}	0.6352	0.7271	0.7011	0.682	0.2267	0.07483	0.004955	0
r_{28}	1.222	1.353	1.298	1.259	0.4534	0.1496	0.009892	0
r_{29}	0.5872	0.6256	0.5968	0.5769	0.2267	0.07478	0.004937	0
r_{30}	0.5872	0.6256	0.5968	0.5769	0.2267	0.07478	0.004937	0
r_{31}	2.336	1.936	1.942	1.922	3.123	3.129	2.652	3.068
r_{32}	2.764	2.347	2.324	2.284	3.315	3.17	2.623	3.068
r_{33}	0.4779	0.6464	0.6464	0.6464	0.1032	0.1032	0.1032	0
r_{34}	0.01394	0.01886	0.01886	0.01886	0.003012	0.003012	0.003012	0
r_{35}	0.1998	0.01779	0.02804	0.03851	0.6906	0.7952	0.8998	1
r_{36}	0.1998	0.01779	0.02804	0.03851	0.6906	0.7952	0.8998	1
r_{37}	0.1998	0.01779	0.02804	0.03851	0.6906	0.7952	0.8998	1
r_{38}	0	0	0	0	0	0	0	0
r_{39}	0	0	0	0	0	0	0	0
r_{40}	0.5576	0.7543	0.7543	0.7543	0.1205	0.1205	0.1205	0
r_{41}	0.4918	0.6653	0.6653	0.6653	0.1063	0.1063	0.1063	0
r_{42}	2.375	2.299	2.266	2.228	2.259	1.864	1.428	1.5
r_{43}	0.8842	0.5562	0.5781	0.5648	1.857	1.506	0.8207	0.867
r_{44}	0.3176	0.3636	0.3505	0.341	0.1134	0.03741	0.002478	0
r_{45}	5.495	5.021	4.856	4.696	5.171	3.353	1.783	2.198

achieved in this test were 0.106 (g/g) for PHB, and 0.33 (g/g) for biomass. The model has resulted with practically identical values. These values are typical for the nutrient balanced growth, because *C. necator* under nitrogen rich conditions dominantly synthesizes biomass and only low quantity of C-source is converted to PHB. Similar results for biomass and PHB yields were achieved also for the batch part of cultivation during start up procedure for five-step continuous cultivation (0.295 g/g for biomass and 0.095 g/g for PHB). The agreement between model and experiment was for the batch parts of both fermentations (A and B) similar as presented in Fig. 5 (results not shown). All this agreements constitute evidence for the validity of the established metabolic network as well as for the appropriateness of the related mathematical model.

Elementary flux modes, yield space analysis and high structured metabolic model combined for analysis of multistage reactor systems were never before described in literature. In general, there is no similar work for analysis of continuous processes, especially not for five-step PHB biosynthesis. Similar flux analysis of metabolism was done for other microorganisms (i.e. PHB non-producer) [62,70] but such work it is rare in the case of *C. necator*. Although Yu and Si [71] have published results dealing with metabolic fluxes for growth of *Ralstonia eutropha* on short chain fatty acids (fed-batch process), and Leonard and Lindley [72] have investigated C-flux for *Alcaligenes eutrophus* grown on phenol in continuous culture. Unfortunately, metabolic fluxes achieved in just mentioned works are not comparable with results in work at hand because of differences in general metabolic situation between two experiments (occurrence of gluconeogenesis, opposite metabolic situation than for growth on glucose). Two related comparable works were published recently: by Park et al. [54] and by Franz et al. [53]. In the last one EMs, yield analysis and model verification for batch cultivation of *C. necator* on fructose was performed, but mentioned authors have used the cybernetic model (not kinetic as is in work at hand). Cybernetic model developed by Franz et al. [53] presents an excellent agreement with experiments but differs to our model adopted for cultivation of the same microorganism on glucose. The complexity of metabolic networks in both models is approximately on the same level. Although both metabolic networks are very close,

Table 3
Metabolic fluxes ([mol S/mol Glu], normalized with respect to glucose uptake) related to different metabolic state of cells in 5-stage reactor cascade system (cultivation A) when r_{11} was assumed to be unidirectional, i.e. positive (direction G6P → F6P).

	Batch	R1 yield			R2 yield			R3 yield
		Lower error value	Experimental value	Upper error value	Lower error value	Experimental value	Upper error value	Lower error value
r_1	1	1	1	1	–	1	1	1
r_2	0.9776	0.9699	0.97	0.97	–	0.9893	0.9943	1
r_3	0.944	0.9233	0.9232	0.9231	–	0.9891	0.9896	1
r_4	0.944	0.9233	0.9232	0.9231	–	0.9891	0.9896	1
r_5	0.03358	0.04666	0.04678	0.04687	–	0.0001127	0.004679	0
r_6	0.05134	0.06986	0.0699	0.06993	–	0.008711	0.01023	0
r_7	−0.01776	−0.0232	−0.02313	−0.02306	–	−0.008598	−0.005554	0
r_8	0.001157	0.001978	0.002015	0.002045	–	−0.002131	−0.0006088	0
r_9	0.001157	0.001978	0.002015	0.002045	–	−0.002131	−0.0006088	0
r_{10}	−0.01892	−0.02518	−0.02514	−0.02511	–	−0.006468	−0.004946	0
r_{11}	0.01069	0.01423	0.01419	0.01414	–	0.008214	0.003155	0
r_{12}	0.01097	0.01425	0.01421	0.0142	–	0.001228	0.003242	0
r_{13}	−0.01097	−0.01425	−0.01421	−0.0142	–	−0.001228	−0.003242	0
r_{14}	−0.01097	−0.01425	−0.01421	−0.0142	–	−0.001228	−0.003242	0
r_{15}	0.8959	0.8598	0.8598	0.8598	–	0.9787	0.9766	1
r_{16}	0.8959	0.8598	0.8598	0.8598	–	0.9787	0.9766	1
r_{17}	0.8123	0.7466	0.7467	0.7467	–	0.9606	0.9586	1
r_{18}	0.8123	0.7466	0.7467	0.7467	–	0.9606	0.9586	1
r_{19}	3.976	3.08	3.001	2.921	–	4.012	3.04	3.5
r_{20}	2.118	1.878	1.855	1.833	–	2.093	1.89	2
r_{21}	0.8025	0.8846	0.864	0.8431	–	0.2312	0.02877	0
r_{22}	0.8025	0.8846	0.864	0.8431	–	0.2312	0.02877	0
r_{23}	0.09451	0.2088	0.2113	0.212	–	0.01277	0.01279	0
r_{24}	0.0354	0.1288	0.1313	0.1321	–	2.275e−006	1.577e−005	0
r_{25}	0.0354	0.1288	0.1313	0.1321	–	2.275e−006	1.577e−005	0
r_{26}	0.7434	0.8046	0.7841	0.7631	–	0.2184	0.016	0
r_{27}	0.7434	0.8046	0.7841	0.7631	–	0.2184	0.016	0
r_{28}	1.451	1.48	1.437	1.394	–	0.4368	0.03199	0
r_{29}	0.708	0.6758	0.6527	0.6311	–	0.2184	0.01599	0
r_{30}	0.708	0.6758	0.6527	0.6311	–	0.2184	0.01599	0
r_{31}	3.644	2.912	2.856	2.798	–	3.873	3.106	3.5
r_{32}	4.193	3.373	3.293	3.214	–	4.057	3.088	3.5
r_{33}	0.4779	0.6464	0.6464	0.6464	–	0.1032	0.1032	0
r_{34}	0.01394	0.01886	0.01886	0.01886	–	0.003012	0.003012	0
r_{35}	0.1998	0.01779	0.02804	0.03851	–	0.7994	0.8998	1
r_{36}	0.1998	0.01779	0.02804	0.03851	–	0.7994	0.8998	1
r_{37}	0.1998	0.01779	0.02804	0.03851	–	0.7994	0.8998	1
r_{38}	0	0	0	0	–	0	0	0
r_{39}	0	0	0	0	–	0	0	0
r_{40}	0.5576	0.7543	0.7543	0.7543	–	0.1205	0.1205	0
r_{41}	0.4918	0.6653	0.6653	0.6653	–	0.1063	0.1063	0
r_{42}	2.321	2.26	2.224	2.188	–	1.773	1.422	1.5
r_{43}	−0.03257	−0.06192	−0.06948	−0.07909	–	−2.528e−006	−0.09081	0
r_{44}	0.3717	0.4023	0.392	0.3816	–	0.1092	0.008001	0
r_{45}	4.793	4.511	4.406	4.297	–	3.873	3.03	3.5

unfortunately the direct comparison of results is not possible (the metabolic fluxes are not presented in details by Franz et al. [53]). In addition, the continuous process as one-step type was performed by Franz et al. only *in silico*. The authors have underlined that application of low dilution rates ($D < 0.08\ h^{-1}$) combined with low substrate load leads imperatively to the incorporation of PHB consumption into modeling. That is in good accordance with results in work at hand: applied dilution rates were in all reactors of 5-stage cascade at least $0.13\ h^{-1}$, so it was reasonable to exclude the PHB degradation from the model because the high substrate load was present. Just mentioned did not cause a negative influence on the agreement between experimental and simulated results. The work of Park et al. [54] is based on kinetic modeling, and the cultivation of *Ralstonia eutropha* was performed in minimal medium. Model RehMBEL 1391 proposed by Park et al. [54] is composed of 1391 reactions, 229 transport reactions and 1171 metabolites in metabolic network. This model suitable for microbiological, genetic and metabolic engineering purposes covers the wider range of possible metabolic situations than the model described in work at hand. The consequences of application of such model in EMs/yield space analysis will be the extraordinary overproduction of EMs, and according to Pinto and Immanuel [73] and Disli et al. [74], the occurrence of multiple mathematical solutions of metabolic steady states for continuous bioreactors. In contrary, the model proposed in the work at hand is more simple and restricted to exponential (nutrient balanced) growth as well as to nitrogen limited, glucose sufficient cultivations (steady state assumptions for metabolic fluxes are valid). Such model quantitatively covers the majority of C and N metabolic fluxes under mentioned cultivation conditions, and therefore is appropriate for industrial cultivations. Among others, the targets of investigation performed by Park et al. [54] were the influences of pH value and C/N ratio for batch cultivation and for one stage chemostat (in dependence on dilution rate). Just mentioned was not the target in our work (for these parameters, optimal values from literature data and from preliminary experiments were applied), the target was to analyze multistage continuous PHB production in order to discover the possible bottlenecks (especially the long term influence of nitrogen limitation). This can be valid for other cultivations in the case of the same microbial production strain as used in the study (*C. necator*) as well as for other microbial PHA-accumulating organisms. Further, the presented approach can be used to comprehend the metabolic ongoings if other substrates

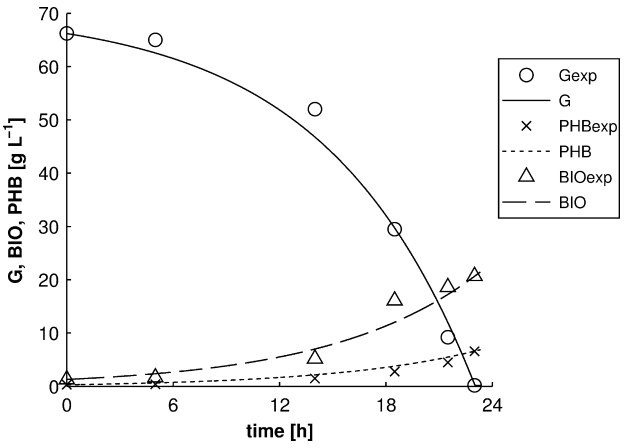

Fig. 5. Experimental and simulated data for nutrient balanced growth of *C. necator* on glucose and ammonia as C- and N-sources (Data are the average values achieved from three parallel cultivations, performed under same conditions).

than glucose are used, e.g. in the case of multi-substrate cultivation for PHA co-polyester production, and especially in the case of sequenced addition of different monomers alongside the reactor cascade. That was the main reason why the five-step cascade was tested (so that model and software systems will be prepared also for the future investigations; in contrary, the same result can be achieved using three-step cascade with larger volume of last reactor). In addition, one must not forget that the presented work only displays the "most simple case" of multistage PHB production by *C. necator* on glucose (as a starting point in development of more complicated sequenced-type multisubstrate cultivations); in future, this can be applied for the deeper understanding of formation of "smart polymeric materials" like PHA-block polymers consisting of hard and soft segments [75,76] (especially here, applying the multistage cascade is a promising strategy), mcl-PHA latexes, and PHAs harboring functional groups. In the latter case, special precursor substrates are required with metabolic routes until the incorporation into the "functional PHA" that are not well described until today.

For above described cases and for highly sophisticated, complex nutrients (e.g. carbon-rich industrial waste streams), further upgrading of the metabolic model will be necessary. In addition, our approach is not restricted to the five-stage continuous system, but will also be valuable for a process-engineering production system with a restricted number of bioreactor vessels. Last, but not least, our approach can be applied to describe multi-step-continuous biotechnological production systems where, similar to the PHA-case, product formation is decoupled from the phase of formation of catalytically active biomass (e.g. secondary metabolites and storage materials like oils composed of special fatty acids, and maybe even in the case of antibiotic production).

The deep understanding of the complex metabolic interrelations of continuous multi-stage PHA production by elementary flux modes, yield space analysis and high structured metabolic modeling is needed to identify bottlenecks in the processes. Dealing with these bottlenecks finally enables to get the required knowledge to implement the system on an industrial scale.

4. Conclusions

The high structured metabolic model for PHB production on glucose by *C. necator* predicts well growth of this microorganism and related PHB synthesis. High structured metabolic model, elementary modes concept and metabolic yield analysis combined for analyzing of multistage continuous production of PHB are a viable and powerful tool for analyzing the metabolic state of cells in different steps of a multistage reactor cascade. This tool can act as a suitable option for detailed optimization of such production systems concerning biomass degradation under long term nitrogen starvation, as it is the case if high PHA productivity is intended. In case of PHB synthesis, all possible metabolic states of cells at different stages of the cascade were evidenced by applying experimental yields and metabolic flux calculations performed by the Metatool software. The cultivation type A (glucose feeding in all reactors) has turned out as the most suitable strategy to perform multistage continuous PHB synthesis.

Acknowledgment

This work was supported by the Collaborative EU FP7 project ANIMPOL ("Biotechnological conversion of carbon containing wastes for eco-efficient production of high added value products"; Grant agreement no.: 245084).

Appendix A. Supplementary data

Supplementary data associated with this article can be found, in the online version, at http://dx.doi.org/10.1016/j.bej.2013.07.003.

References

[1] Y. Doi, A. Steinbüchel (Eds.), Biopolymers, vol. 3b: Polyesters, Wiley-VCH, Weinheim, 2001, p. 480.
[2] M. Koller, A. Salerno, M. Dias, A. Reiterer, G. Braunegg, Modern biotechnological polymer synthesis—a review, Food Technol. Biotechnol. 48 (2010) 255–269.
[3] A. Steinbüchel, H.G. Schlegel, Physiology and molecular genetics of poly(b-hydroxyalkanoic acid) synthesis in *Alcaligenes eutrophus*, Mol. Microbiol. 5 (1991) 535–542.
[4] M. Koller, I. Gasser, F. Schmid, G. Berg, Linking ecology with economy: insights into polyhydroxyalkanoate-producing microorganisms, Eng. Life Sci. 11 (2011) 222–237.
[5] A. Steinbüchel, B. Füchtenbusch, Bacterial and other biological systems for polyester production, Trends Biotechnol. 16 (1998) 419–427.
[6] G. Braunegg, M. Koller, P. Varila, C. Kutschera, R. Bona, C. Hermann, P. Horvat, J. Neto, L. Pereira, Production of plastics from waste derived from agrofood industry, in: P. Fornasiero, M. Graziani (Eds.), Renewable Resources and Renewable Energy, University of Trieste, Trieste, 2007, pp. 119–135.
[7] S.Y. Lee, Plastic bacteria? Progress and prospects for polyhydroxyalkanoate production in bacteria, Trends Biotechnol. 14 (1996) 431–438.
[8] S.Y. Lee, Bacterial polyhydroxyalkanoates, Biotechnol. Bioeng. 49 (1996) 1–14.
[9] G.Q. Chen, A microbial polyhydroxyalkanoates (PHA) based bio- and materials industry, Chem. Soc. Rev. 38 (2009) 2434–2446.
[10] S. Khanna, A. Srivastava, Recent advances in microbial polyhydroxyalkanoates, Process Biochem. 40 (2005) 607–619.
[11] C.S.K. Reddy, R. Ghai, K.V.C. Rashmi, Polyhydroxyalkanoates: an overview, Bioresour. Technol. 87 (2003) 137–146.
[12] Q. Ren, A. Grubelnik, M. Hoerler, K. Ruth, R. Hartmann, H. Felber, M. Zinn, Bacterial poly(hydroxyalkanoates) as a source of chiral hydroxyalkanoic acids, Biomacromolecules 6 (2005) 2290–2298.
[13] J. Choi, S.Y. Lee, Factors affecting the economics of polyhydroxyalkanoate production by bacterial fermentation, Appl. Microbiol. Biotechnol. 51 (1999) 13–21.
[14] M. Koller, P. Hesse, C. Kutschera, R. Bona, J. Nascimento, S. Ortega, J. Agnelli, G. Braunegg, Sustainable embedding of the bioplastic poly-(3-hydroxybutyrate) into sugarcane industry: principles of a future-oriented technology in Brazil. Polymers—Opportunities and Risks, vol. II, Springer-Verlag, Berlin Heidelberg, 2010, pp. 81–96.
[15] K. Sudesh, T. Iwata, Sustainability of biobased and biodegradable plastics, Clean Soil Air Water 36 (2008) 433–442, http://dx.doi.org/10.1002/clen.200700183.
[16] B.A. Ramsay, K. Lomaliza, C. Chavarie, B. Dubé, P. Bataille, J.A. Ramsay, Production of poly-(b-hydroxybutyric-co-bhydroxyvaleric) acids, Appl. Environ. Microbiol. 56 (1990) 2093–2098.
[17] J.F. Wilkinson, A.L.S. Munro, Influence of growth-limiting conditions on the synthesis of possible carbon and energy storage polymers in *Bacillus megaterium*, in: E.O. Powell, C.G.T. Evans, R.E. Strange, D.W. Tempest (Eds.), Microbial Physiology and Continuous Culture, HMSO, London, 1967, pp. 173–185.
[18] N. Koyama, Y. Doi, Continuous production of poly(3-hydroxybutyrate-co-3-hydroxyvalerate) by *Alcaligenes eutrophus*, Biotechnol. Lett. 17 (1995) 281–284.
[19] S.T. Yu, C.C. Lin, J.R. Too, PHBV production by *Ralstonia eutropha* in a continuous stirred tank reactor, Process Biochem. 40 (2005) 2729–2734.
[20] G. Braunegg, K. Genser, R. Bona, G. Haage, F. Schellauf, E. Winkler, Production of PHAs from agricultural waste material, Macromol. Symp. 144 (1999) 375–383.

[21] G. Braunegg, G. Lefebvre, G. Renner, A. Zeiser, G. Haage, K. Loidl-Lanthaler, Kinetics as a tool for polyhydroxyalkanoate production optimization, Can. J. Microbiol. 41 (1995) 239–248.
[22] R. Hartmann, R. Hany, E. Pletscher, A. Ritter, B. Witholt, M. Zinn, Tailor-made olefinic medium-chain-length poly-[(R)-3-hydroxyalkanoates] by *Pseudomonas putida* GPo1: batch versus chemostat production, Biotechnol. Bioeng. 93 (2001) 737–746.
[23] R. Hartmann, R. Hany, T. Geiger, T. Egli, B. Witholt, M. Zinn, Tailored biosynthesis of olefinic medium-chain-lengthpoly[(R)-3-hydroxyalkanoates] in *Pseudomonas putida* GPo1with improved thermal properties, Macromolecules 37 (2004) 6780–6785.
[24] J.U. Ackermann, W. Babel, Approaches to increase the economy of the PHB production, Polym. Degrad. Stab. 59 (1998) 183–186.
[25] W. Babel, J.U. Ackermann, U. Breuer, Physiology, regulation, and limits of the synthesis of poly(3HB), in: W. Babel, A. Steinbüchel (Eds.), Advances in Biochemical Engineering/Biotechnology (Biopolyesters), vol. 71, Springer-Verlag, Berlin Heidelberg, 2001, pp. 125–157.
[26] G. Du, J. Chen, J. Yu, S. Lun, Continuous production of poly-3-hydroxybutyrate by *Ralstonia eutropha* in a two-stage culture system, J. Biotechnol. 88 (2001) 59–65.
[27] G. Du, J. Chen, J. Yu, S. Lun, Kinetic studies on poly-3-hydroxybutyrate formation by Ralstonia eutropha in a two-stage continuous culture system, Process Biochem. 37 (2001) 219–227.
[28] G. Mothes, J.U. Ackermann, Synthesis of poly(3-hydroxybutyrateco-4-hydroxybutyrate) with a target mole fraction of 4-hydroxybutyric acid units by two-stage continuous cultivation of *Delftia acidovorans* P4a, Eng. Life Sci. 5 (2005) 58–62.
[29] M. Zinn, H.U. Weilenmann, R. Hany, M. Schmid, T. Egli, Tailored synthesis of poly([R]-3-hydroxybutyrate-co-3-hydroxyvalerate) (PHB/HV) in *Ralstonia eutropha* DSM 428, Acta Biotechnol. 23 (2003) 309–316.
[30] M. Zinn, B. Witholt, T. Egli, Dual nutrient limited growth: models, experimental observations, and applications, J. Biotechnol. 113 (2004) 263–279.
[31] T. Egli, On multiple-nutrient-limited growth of microorganisms, with special reference to dual limitation by carbon and nitrogen substrates, Antonie Van Leeuwenhoek 60 (1991) 225–234.
[32] T. Egli, J.R. Quayle, Influence of the carbon: nitrogen ratio of the growth medium on the cellular composition and ability of the methylotrophic yeast *Hansenula polymorpha* to utilize mixed carbon sources, J. Gen. Microbiol. 132 (1986) 1779–1788.
[33] S.T. Wu, Y.C. Lin, J.R. Too, Continuous production of poly(3-hydroxybutyrate-co-3-hydroxyvalerate): effects of C/N ratio and dilution rate on HB/HV ratio, Korean J. Chem. Eng. 26 (2009) 411–416.
[34] A. Atlić, M. Koller, D. Scherzer, C. Kutschera, E. Grillo-Fernandes, P. Horvat, E. Chiellini, G. Braunegg, Continuous production of poly([R]-3-hydroxybutyrate) by *Cupriavidus necator* in a multistage bioreactor cascade, Appl. Microbiol. Biotechnol. 91 (2) (2011) 295–304.
[35] E.N. Pederson, C.W.J. McChalicher, F. Srienc, Bacterial synthesis of PHA block copolymers, Biomacromolecules 7 (2006) 1904–1911.
[36] P. Horvat, I. Vrana Špoljarić, M. Lopar, A. Atlić, M. Koller, G. Braunegg, Mathematical modelling and process optimization of a continuous 5-stage bioreactor cascade for production of poly[-(R)-3-hydroxybutyrate] by *Cupriavidus necator*, Biopr. Biosyst. Eng. (2012), online ahead of press; http://dx.doi.org/10.1007/s00449-012-0852-8
[37] G.N. Stephanopoulos, A.A. Aristidou, J. Nielsen, Metabolic Engineering: Principles and Methodologies, Academic Press, San Diego, 1998, pp. 725.
[38] A.K. Gombert, J. Nielsen, Mathematical modeling of metabolism, Curr. Opin. Biotechnol. 11 (2000) 180–186.
[39] A. Varma, B.Ø. Palsson, Stoichiometric flux balance models quantitatively predict growth and metabolic by-product secretion in wild-type *Escherichia coli* W3110, Appl. Environm. Microbiol. 60 (1994) 3724–3731.
[40] J.S. Edwards, R. Ramakrishna, C.H. Schilling, B.O. Palsson, Metabolic flux balance analysis, in: S.Y. Lee, E.T. Papoutsakis (Eds.), Metabolic Engineering, Marcel Deker, New York, 1999, pp. 13–57.
[41] J. Stelling, S. Klamt, K. Bettenbrock, S. Schuster, E.D. Gilles, Metabolic network structure determines key aspects of functionality and regulation, Nature 420 (2002) 190–1933.
[42] S. Schuster, D.A. Fell, T. Dandekar, A general definition of metabolic pathways useful for systematic organization and analysis of complex metabolic networks, Nat. Biotechnol. 18 (2000) 326–332.
[43] J.A. Papin, J. Stelling, N.D. Price, S. Klamt, S. Schuster, B.Ø. Palsson, Comparison of network-based pathway analysis methods, Trends Biotechnol. 22 (2004) 400–405.
[44] J.A. Papin, N.D. Price, B.Ø. Palsson, Extreme pathway lengths and reaction participation in genome-scale metabolic networks, Genome Res. 12 (2002) 1889–1900.
[45] N.D. Price, J.A. Papin, C.H. Schilling, O. Bernhard, B.O. Palsson, Genome-scale microbial in silico models: the constraints-based approach, Trends Biotechnol. 21 (2003) 162–169.
[46] M.E. Bushell, S.I.P. Sequeira, C. Khannapho, H. Zhao, K.F. Chater, M.J. Butler, A.M. Kierzek, C.A. Avignone-Rossa, The use of genome scale metabolic flux variability analysis for process feed formulation based on an investigation of the effects of the zwf mutation on antibiotic production in *Streptomyces coelicolor*, Enzyme Microb. Technol. 39 (2006) 1347–1353.
[47] J.M. Park, T.Y. Kim, S.Y. Lee, Prediction of metabolic fluxes by incorporating genomic context and flux-converging pattern analyses, Proc. Natl. Acad. Sci. U.S.A. 107 (2010) 14931–14936.
[48] A. Larhlimi, A. Bockmayr, A new constraint-based description of the steady-state flux cone of metabolic networks, Discrete Appl. Math. 157 (2009) 2257–2266.
[49] A. Dräger, M. Kronfeld, M.J. Ziller, J. Supper, H. Planatscher, J.B. Magnus, M. Oldiges, O. Kohlbacher, A. Zell, Modeling metabolic networks in *C. glutamicum*: a comparison of rate laws in combination with various parameter optimization strategies, BMC Syst. Biol. 3 (2009) 5 http://dx.doi.org/10.1186/1752-0509-3-5
[50] H.S. Song, D. Ramkrishna, Reduction of a set of elementary modes using yield analysis, Biotechnol. Bioeng. 102 (2009) 554–568.
[51] A. Pohlmann, W.F. Fricke, F. Reinecke, B. Kusian, H. Liesegang, R. Cramm, T. Eitinger, C. Ewering, M. Pötter, E. Schwartz, A. Strittmatter, I. Voss, G. Gottschalk, A. Steinbüchel, B. Friedrich, B. Bowien, Genome sequence of the bioplastic-producing Knallgas bacterium *Ralstonia eutropha* H16, Nat. Biotechnol. 24 (2006) 1257–1262.
[52] M. Raberg, K. Peplinski, S. Heiss, A. Ehrenreich, B. Voigt, C. Döring, M. Bömeke, M. Hecker, A. Steinbüchel, Proteomic and transcriptomic elucidation of the mutant *Ralstonia eutropha* G + 1 with regard to glucose utilization, Appl. Environ. Microbiol. 77 (2011) 2058–2070.
[53] A. Franz, H.S. Song, D. Ramkrishna, A. Kienle, Experimental, theoretical analysis of poly(β-hydroxybutyrate) formation and consumption in *Ralstonia eutropha*, Biochem. Eng. J. 55 (2011) 49–58.
[54] J.M. Park, T.Y. Kim, S.Y. Lee, Genome-scale reconstruction and in silico analysis of the *Ralstonia eutropha* H16 for polyhydroxyalkanoate synthesis, litoautotrophic growth, and 2-methyl citric acid production, BMC Syst. Biol. 5 (2011) 101.
[55] T. Pfeiffer, I. Sánchez-Valdenebro, J.C. Nuño, F. Montero, S. Schuster, METATOOL: for studying metabolic networks, Bioinformatics 15 (1999) 251–257.
[56] S. Schuster, T. Dandekar, D.A. Fell, Detection of elementary flux modes in biochemical networks: a promising tool for pathway analysis and metabolic engineering, Trends Biotechnol. 17 (1999) 53–60.
[57] J.M. Schwartz, M. Kanehisa, A quadratic programming approach for decomposing steady-state metabolic flux distributions onto elementary modes, Bioinformatics 21 (suppl. 2) (2005) ii204–ii205, http://dx.doi.org/10.1093/bioinformatics/bti1132.
[58] M.G. Poolman, K.V. Venkatesh, M.K. Pidcock, D.A. Fell, A method for the determination of flux in elementary modes, and its application to *Lactobacillus rhamnosus*, Biotechnol. Bioeng. 88 (2004) 601–612.
[59] M.M. Altintas, C.K. Eddy, M. Zhang, J.D. McMillan, D.S. Kompala, Kinetic modeling to optimize pentose fermentation in *Zymomonas mobilis*, Biotechnol. Bioeng. 94 (2006) 273–295.
[60] F.J. Bruggeman, F.C. Boogerd, H.V. Westerhoff, The multifarious short-term regulation of ammonium assimilation of *Escherichia coli*: dissection using an in silico replica, FEBS J. 272 (2005) 1965–1985.
[61] K.L. Burns, C.D. Oldham, J.R. Thompson, M. Lubarsky, S.W. May, Analysis of the in vitro biocatalytic production of poly-(β)-hydroxybutyric acid, Enzyme Microb. Technol. 41 (2007) 591–599.
[62] C. Chassagnole, N. Noisommit-Rizzi, J.W. Schmid, K. Mauch, M. Reuss, Dynamic modeling of the central carbon metabolism of *Escherichia coli*, Biotechnol. Bioeng. 79 (2002) 53–73.
[63] M.H. Hoefnagel, M.J. Starrenburg, D.E. Martens, J. Hugenholtz, M. Kleerebezem, I.I. van Swam, R. Bongers, H.V. Westerhoff, J.L. Snoep, Metabolic engineering of lactic acid bacteria, the combined approach: kinetic modelling, metabolic control and experimental analysis, Microbiology 148 (2002) 1003–1013.
[64] H. Shi, M. Shiraishi, K. Shimizu, Metabolic flux analysis for biosynthesis of poly(β-hydroxybutyric acid) in *Alcaligenes eutrophus* from various carbon sources, J. Ferment. Bioeng. 84 (1997) 579–587.
[65] Y. Usuda, Y. Nishio, S. Iwatani, S.J. van Dien, A. Imaizumi, K. Shimbo, N. Kageyama, D. Iwahata, H. Miyano, K. Matsui, Dynamic modeling of *Escherichia coli* metabolic and regulatory systems for amino-acid production, J. Biotechnol. 147 (2010) 17–30.
[66] C. Yang, Q. Hua, T. Baba, H. Mori, K. Shimizu, Analysis of *Escherichia coli* anaplerotic metabolism and its regulation mechanisms from the metabolic responses to altered dilution rates and phosphoenolpyruvate carboxykinase knockout, Biotechnol. Bioeng. 84 (2003) 129–144.
[67] J. Yuan, C.D. Doucette, W.U. Fowler, X.J. Feng, M. Piazza, H.A. Rabitz, N.S. Wingreen, J.D. Rabinowitz, Metabolomics-driven quantitative analysis of ammonia assimilation in *E. coli*, Mol. Syst. Biol. 5 (2009) 302, http://dx.doi.org/10.1038/msb.2009.60.
[68] A. Kamp, S. Schuster, Metatool 5.0: fast and flexible elementary modes analysis, Bioinformatics 22 (2006) 1930–1931.
[69] T. Katoh, D. Yuguchi, H. Yoshii, H. Shi, K. Shimizu, Dynamics and modeling on fermentative production of poly (β-hydroxybutyric acid) from sugars via lactate by a mixed culture of *Lactobacillus delbrueckii* and *Alcaligenes eutrophus*, J. Biotechnol. 67 (1999) 113–134.
[70] A. Kayser, J. Weber, V. Hecht, U. Rinas, Metabolic flux analysis of *Escherichia coli* in glucose-limited continuous culture. I. Growth-rate-dependent metabolic efficiency at steady state, Microbiology 151 (2005) 693–706.
[71] J. Yu, Y. Si, Metabolic carbon fluxes and biosynthesis of polyhydroxyalkanoates in *Ralstonia eutropha* on short chain fatty acids, Biotechnol. Prog. 20 (2004) 1015–1024.
[72] D. Leonard, N.D. Lindley, Carbon and energy flux constraints in continuous cultures of *Alcaligenes eutrophus* grown on phenol, Microbiology 144 (1998) 241–248.

[73] M.A. Pinto, C.D. Immanuel, Sensitivity of bifurcation traits to model parameters in poly-beta-hydroxy butyrate production, ADCHEM (2006) 103–108.
[74] I. Disli, A. Kremling, A. Kienle, A model based analysis of multiple steady states in continuous cell cultures, in: Proceedings MATHMOD 09 Vienna—Full Papers CD Volume, 2009.
[75] N.V. Mantzaris, A.S. Kelly, P. Daoutidis, F. Srienc, An optimal carbon source switching strategy for the production of PHA di-block copolymers with *Ralstonia eutropha*, A.I.Ch.E. J. 47 (2001) 727–743.
[76] N.V. Mantzaris, A.S. Kelly, P. Daoutidis, F. Srienc, A population balance model describing the dynamics of molecular weight distributions and the structure of PHA copolymer chains, Chem. Eng. Sci. 57 (2002) 4643–4663.